ChemComm

COMMUNICATION

View Article Online
View Journal | View Issue

Cite this: *Chem. Commun.*, 2018, **54**, 13575

Received 25th September 2018,
Accepted 26th October 2018

DOI: 10.1039/c8cc07405d

rsc.li/chemcomm

Spiro-fused bis-hexa-*peri*-hexabenzocoronene†

Yunbin Hu,[ab] Di Wang,[a] Martin Baumgarten,[a] Dieter Schollmeyer,[c] Klaus Müllen*[a] and Akimitsu Narita*[a]

A spiro-fused hexa-*peri*-hexabenzocoronene dimer was synthesized, and its physicochemical properties were studied by UV-Vis absorption and emission spectroscopy as well as cyclic voltammetry. Chemical oxidation of SB-HBC afforded its radical cation and dication derivatives, which could be reversibly reduced to the neutral state.

Spiro-fused polycyclic aromatic compounds, in which orthogonal π-systems are linked by a common sp^3-hybridized atom, have been widely investigated due to their three-dimensional (3D) geometries, high thermal stability, good processability and unique spiro-conjugation effects.[1,2] Spirobifluorene (SBF) represents the most studied class of spiro-conjugated molecules, which has been recognized as a promising building block for functional materials in organic light-emitting diodes, phototransistors and solar cells.[3–11] The structural modification of SBF has been achieved by core-substitution at the 3,6- and/or 2,7-positions aiming at tuning the optical and electronic properties (Fig. 1).[12–19] However, much less effort has been devoted to extend the π-system of SBF by annulation with aromatic units (Fig. 1),[20–23] although this can lead to rigid and enlarged spiro π-systems with increased intermolecular π–π overlap in the solid state.[24] In particular, the core-annulation at 3, 4, 5, and 6 positions of SBF that enables the construction of spiro-fused large polycyclic aromatic hydrocarbons (PAHs) has remained elusive (Fig. 1).[25]

Hexa-*peri*-hexabenzocoronene (HBC) is an intriguing PAH with a large π-system which gives rise to a pronounced self-assembly and high intrinsic charge-carrier mobility.[25,26] There are numerous planar HBC derivatives in the literature, but there has been only a limited number of reports on the incorporation of HBC into 3D scaffolds,[27–29] despite the intriguing properties demonstrated for smaller PAHs arranged in 3D structures, such as intrinsic chirality,[30,31] amorphous aggregation[1] and unique packing modes.[32,33] Herein, we report an efficient synthesis of a novel 3,4,5,6-annulated SBF derivative, bearing two spiro-linked HBC units (spiro-bis-HBC, **SB-HBC**, Scheme 1). Its robust orthogonally arranged structure was confirmed by X-ray crystallography. The photophysical and electrochemical properties of **SB-HBC** were investigated in comparison with the parent HBC, revealing largely enhanced absorptivity and two-electron oxidation. Moreover, chemical oxidation and reduction were shown to be reversible.

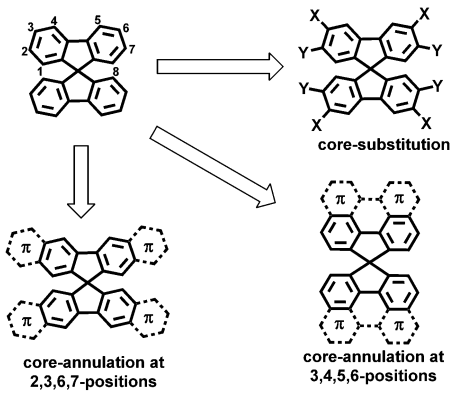

Fig. 1 Functionalization of spirobifluorene.

The synthesis of **SB-HBC** is depicted in Scheme 1. Starting from 4,4′-dibromo-9,9′-spirobifluorene (**1**),[34] a two-fold palladium-catalyzed Sonogashira coupling of **1** with trimethylsilylacetylene was performed in the presence of tetrakis(triphenylphosphine)-palladium ($Pd(PPh_3)_4$) and copper(I) iodide (CuI) in piperidine, affording 4,4′-bis(trimethylsilylethynyl)-9,9′-spirobifluorene **2** in 86% yield. The relatively high reaction temperature (120 °C) was necessary to overcome the steric hindrance at the bay

[a] *Max-Planck-Institut für Polymerforschung, Ackermannweg 10, 55128 Mainz, Germany. E-mail: muellen@mpip-mainz.mpg.de, narita@mpip-mainz.mpg.de*
[b] *Department of Organic and Polymer Chemistry, College of Chemistry and Chemical Engineering, Central South University, Changsha, Hunan 410083, P. R. China*
[c] *Institut für Organische Chemie, Johannes Gutenberg-Universität Mainz, Duesbergweg 10-14, 55099 Mainz, Germany*

† Electronic supplementary information (ESI) available: Materials and methods, syntheses, spectra, properties, characterization data and structures, including Fig. S1–S23 and Tables S1 and S2. CCDC 1848515. For ESI and crystallographic data in CIF or other electronic format see DOI: 10.1039/c8cc07405d

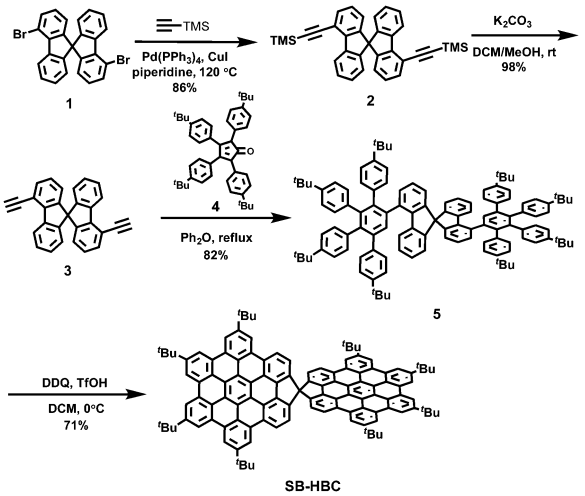

Scheme 1 Synthesis of spiro-fused bis-HBC (**SB-HBC**).

positions of **1**. Then, the trimethylsilyl groups were removed upon treatment of **2** with potassium carbonate (K_2CO_3) in dichloromethane (DCM) and methanol (MeOH), furnishing 4,4′-diethynyl-9,9′-spirobifluorene (**3**) in 98% yield. Bisdienophile **3** was then subjected to a two-fold Diels–Alder reaction with cyclopentadienone **4**, providing the spirobifluorene-based polyphenylene precursor **5** in 82% yield. The final oxidative cyclodehydrogenation of **5** resulted in the formation of spiro-fused HBC dimer **SB-HBC** as a yellow solid in 71% yield. The chemical structure of **SB-HBC** was unambiguously disclosed by mass and NMR spectroscopies as well as X-ray crystallography. It is noteworthy that well-resolved ^{1}H-NMR spectrum of **SB-HBC** was recorded, where all the aromatic protons could be clearly assigned by ^{1}H–^{1}H correlation spectroscopy (COSY) and nuclear overhauser enhancement spectroscopy (NOESY) measurements (see ESI† for further details).

Single crystals of **SB-HBC** were grown by slowly diffusing pentane vapor into its tetrahydrofuran solution. As shown in Fig. 2, the **SB-HBC** molecule revealed a nearly orthogonal spiro-shaped structure with the dihedral angle of 87.0° between the two fused five-membered rings. This is close to the reported torsion angle of SBF (*ca.* 89.0°)[35] and also in good agreement with the value of 88.7° calculated for the gas phase by density functional theory (DFT) at the B3LYP/6-31G(d,p) level (Fig. S2, ESI†). The HBC subunits in **SB-HBC** are slightly bent, with the largest distance of 0.48 Å between the outermost carbons and the plane of the central benzene ring. This is attributed to the concurrent effects of the steric interactions among *tert*-butyl groups and the strains induced by the five-membered rings. It is noteworthy that adjacent **SB-HBC** molecules are stacked by π–π overlap of the HBC subunits along the *c*-axis, forming one-dimensional arrays (Fig. 2c). The intermolecular π–π stacking distances are in the range of 3.42 to 3.63 Å. This molecular stacking mode is similar to that of previously reported spirobiphenalenyl neutral radicals, which show long-range one-dimensional charge-transporting properties.[36,37]

The optoelectronic behavior of **SB-HBC** was initially investigated by UV-Vis absorption spectroscopy in comparison with

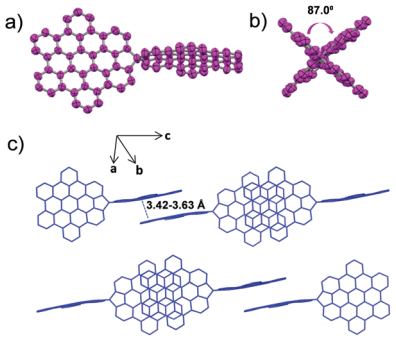

Fig. 2 Crystal structure of **SB-HBC**. Solvent molecules, *tert*-butyl groups, and hydrogen atoms were omitted for clarity. (a) Top view and (b) side view. Thermal ellipsoids are shown at 50% probability. (c) Molecular packing of **SB-HBC** in one unit cell.

2,5,8,11,14,17-hexa-*tert*-butyl-HBC (**HBC-*t*Bu**).[38,39] As displayed in Fig. 3a, **SB-HBC** exhibits a similar but less structured absorption pattern. The significantly enhanced absorption behavior of **SB-HBC** relative to **HBC-*t*Bu** can be clearly disclosed from the nearly two-fold enhancement of the maximum molar extinction coefficient (ε_{max}(**SB-HBC**) at 363 nm: ~3.1 × 10^5 L mol^{-1} cm^{-1} and ε_{max}(**HBC-*t*Bu**) at 359 nm: ~1.8 × 10^5 L mol^{-1} cm^{-1}). The slightly red-shifted absorption maximum of SB-HBC implied the spiro-conjugation effect between two spiro-fused HBC moieties, which has been previously observed in other spirocyclic fused aromatics.[24] Further lower-energy absorption bands for **SB-HBC** were observed at 432 nm (ε: ~6.0 × 10^3 L mol^{-1} cm^{-1}) with a shoulder at 442 nm and at 464 nm (ε: ~6.3 × 10^3 L mol^{-1} cm^{-1}), which are more pronounced compared with the corresponding

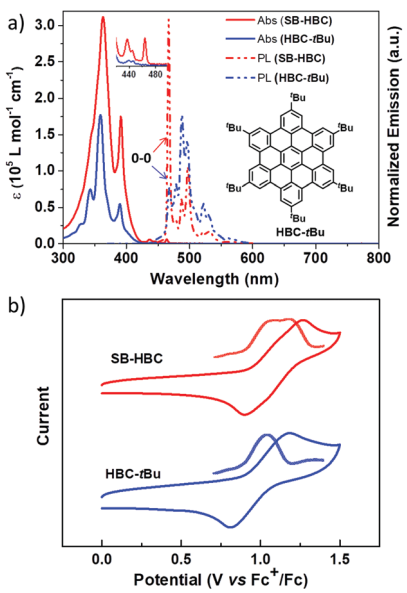

Fig. 3 (a) UV-Vis absorption (Abs) and photoluminescence (PL) spectra (0–0 vibronic transitions are notified with arrows) of 5.0 × 10^{-6} mol L^{-1} **SB-HBC** and **HBC-*t*Bu** in DCM. Inset: Magnified absorption region for better visualization. (b) Cyclic voltammetry and differential pulse voltammetry profiles of 1.0 × 10^{-3} mol L^{-1} **SB-HBC** and **HBC-*t*Bu** in 1,1,2,2-tetrachloroethane.

peaks from **HBC-*t*Bu** (inset Fig. 3a). Excitation spectrum of **SB-HBC** is well consistent with the absorption with distinct long-wavelength excitation bands at 438, 446 and 465 nm (Fig. S6, ESI†). Notably, compared to **HBC-*t*Bu**, **SB-HBC** showed an extremely sharp emission band at 467 nm assignable to the 0–0 vibronic transition (Fig. 2a), which is attributed to a reduced symmetry of **SB-HBC**.[40] Furthermore, the fluorescence quantum yield of **SB-HBC** was determined to be 0.063, which is higher than the reported values of **HBC-*t*Bu** (Φ_F = 0.030) and other alkyl substituted HBC derivatives.[41] In contrast to the doubly degenerated HOMO and LUMO of unsubstituted HBC, DFT calculations demonstrated the non-degenerate frontier molecular orbitals (HOMO and LUMO) of **SB-HBC**, with the electron density shared over the spiro bridge (Fig. 4). On the basis of the time-dependent DFT (TD-DFT) method, HBC shows a symmetry-forbidden low-energy transition at 429 nm (oscillator strength (f) = 0.000) (Fig. S4 and Table S1, ESI†), which was previously assigned to the α-band.[42] In contrast, the low-energy transition at 432 nm of **SB-HBC** is partially symmetry allowed with f = 0.023 (Fig. S5 and Table S2, ESI†), which is in line with the experimental observations. When studied by cyclic voltammetry, **SB-HBC** presented reversible two-electron oxidation in the range of 0–1.5 V as evidenced by differential pulse voltammetry (DPV) curves in contrast to the one-electron oxidation process of **HBC-*t*Bu** (Fig. 3b). The onset oxidation potentials of **SB-HBC** and **HBC-*t*Bu** were close to each other (**SB-HBC**: 0.95 V, **HBC-*t*Bu**: 0.92 V), which implied their comparable electron-donating abilities.

We also undertook chemical oxidation of **SB-HBC** using antimony chloride ($SbCl_5$) as the oxidant, which were monitored by UV-Vis-NIR absorption spectroscopy and electron paramagnetic resonance (EPR) measurements. Upon incremental addition of a solution of $SbCl_5$ in DCM, the light yellow solution of **SB-HBC** turned red with the appearance of a sharp absorption band at 548 nm and a broad band from 600 to 1000 nm centered at 815 nm (red lines in Fig. 5a). We assign these new absorption bands to the radical cation of **SB-HBC** (**SB-HBC**$^{\bullet+}$), also based on the observation of an intensive EPR signal (g = 2.0033) (inset of Fig. 5a and Fig. S8, S9, ESI†). Excess amounts of $SbCl_5$ were necessary for this oxidation process (Fig. S7, ESI†). Nevertheless, loss of degeneracy in the HOMO of **SB-HBC**, as predicted by the DFT calculation (Fig. 4), precludes the formation of bis(radical cation) species.

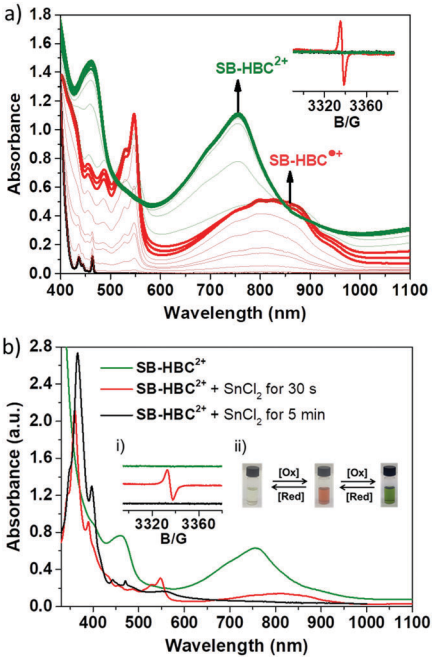

Fig. 5 (a) Absorption and EPR (displayed in the inset) spectral changes upon the oxidation of **SB-HBC** (2.0×10^{-5} mol L^{-1} in DCM) by incremental addition of $SbCl_5$. (b) Absorption and EPR (displayed in inset i) spectral changes of **SB-HBC**$^{2+}$ in DCM (1×10^{-5} mol L^{-1}) after the addition of excessive $SnCl_2$ for the indicated time. Inset ii: Photographs of **SB-HBC** in DCM observed upon the oxidation by $SbCl_5$ followed with the reduction by $SnCl_2$.

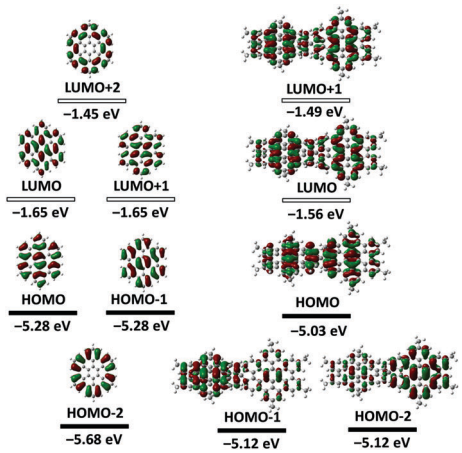

Fig. 4 Energies and shapes of frontier orbitals of HBC and model **SB-HBC** at the B3LYP/6-31G level of theory.

Further oxidation of the red **SB-HBC**$^{\bullet+}$ with an increasing amount of $SbCl_5$ afforded a green solution with a broad absorption band centered at 756 nm (green lines in Fig. 5a). These spectral and color changes coincided with the disappearance of the EPR signal (inset of Fig. 5a), suggesting the formation of diamagnetic **SB-HBC** dication (**SB-HBC**$^{2+}$). This is in agreement with the loss of degeneracy of the HOMO mentioned above and in contrast to oxidation of coronene which can form a paramagnetic diradical dication due to the two-fold degenerate HOMOs.[43]

It is noteworthy that the green **SB-HBC**$^{2+}$ could be reversibly reduced to the neutral state by adding tin(II) chloride ($SnCl_2$). A stepwise color change was observed from green to red and then to light yellow, which was accompanied by simultaneous changes of the absorption and EPR spectra, demonstrating the recovery of **SB-HBC**$^{\bullet+}$ and then of the neutral **SB-HBC** (Fig. 5b). The reversible redox property of **SB-HBC** indicated the good stability of its oxidized species.

In summary, we have demonstrated the efficient synthesis of a spiro-fused bis-HBC (**SB-HBC**), representing a novel PAH with a robust spiro-linkage. The orthogonally arranged π-system of **SB-HBC** was proven by X-ray crystallography, with the adjacent molecules stacking by the marked one-dimensional π–π

overlapping pattern. The chemical oxidation of **SB-HBC** into the stable oxidized species and reversible reduction process are demonstrated. Our result sheds light on π-extended SBF with modulated optical and electronic properties, and can become a starting point for the investigation of other spiro-fused nanographene structures.

We acknowledge the financial support from the Max Planck Society and the European Commission through the FET-Proactive Project "MoQuaS" (No. 610449) and Graphene Flagship (No. CNECT-ICT-604391). Open Access funding provided by the Max Planck Society.

Conflicts of interest

There are no conflicts to declare.

Notes and references

1 T. P. I. Saragi, T. Spehr, A. Siebert, T. Fuhrmann-Lieker and J. Salbeck, *Chem. Rev.*, 2007, **107**, 1011–1065.
2 C. Poriel and J. Rault-Berthelot, *J. Mater. Chem. C*, 2017, **5**, 3869–3897.
3 C. Quinton, S. Thiery, O. Jeannin, D. Tondelier, B. Geffroy, E. Jacques, J. Rault-Berthelot and C. Poriel, *ACS Appl. Mater. Interfaces*, 2017, **9**, 6194–6206.
4 Z. Jiang, H. Yao, Z. Zhang, C. Yang, Z. Liu, Y. Tao, J. Qin and D. Ma, *Org. Lett.*, 2009, **11**, 2607–2610.
5 S. Thiery, D. Tondelier, C. Dedairieux, B. Geffroy, O. Jeannin, R. Metivier, J. Rault-Berthelot and C. Poriel, *J. Phys. Chem. C*, 2015, **119**, 5790–5805.
6 Y.-L. Liao, W.-Y. Hung, T.-H. Hou, C.-Y. Lin and K.-T. Wong, *Chem. Mater.*, 2007, **19**, 6350–6357.
7 T. P. I. Saragi, R. Pudzich, T. Fuhrmann and J. Salbeck, *Appl. Phys. Lett.*, 2004, **84**, 2334–2336.
8 T. P. Osedach, S. M. Geyer, J. C. Ho, A. C. Arango, M. G. Bawendi and V. Bulović, *Appl. Phys. Lett.*, 2009, **94**, 043307.
9 T. P. I. Saragi, R. Pudzich, T. Fuhrmann-Lieker and J. Salbeck, *Opt. Mater.*, 2007, **29**, 879–884.
10 X.-F. Wu, W.-F. Fu, Z. Xu, M. Shi, F. Liu, H.-Z. Chen, J.-H. Wan and T. P. Russell, *Adv. Funct. Mater.*, 2015, **25**, 5954–5966.
11 W. H. Nguyen, C. D. Bailie, E. L. Unger and M. D. McGehee, *J. Am. Chem. Soc.*, 2014, **136**, 10996–11001.
12 U. Bach, D. Lupo, P. Comte, J. E. Moser, F. Weissörtel, J. Salbeck, H. Spreitzer and M. Grätzel, *Nature*, 1998, **395**, 583–585.
13 J.-H. Fournier, T. Maris and J. D. Wuest, *J. Org. Chem.*, 2004, **69**, 1762–1775.
14 K. C. Song, R. Singh, J. Lee, D. H. Sin, H. Lee and K. Cho, *J. Mater. Chem. C*, 2016, **4**, 10610–10615.
15 N. J. Jeon, H. G. Lee, Y. C. Kim, J. Seo, J. H. Noh, J. Lee and S. I. Seok, *J. Am. Chem. Soc.*, 2014, **136**, 7837–7840.
16 L. E. Polander, P. Pahner, M. Schwarze, M. Saalfrank, C. Koerner and K. Leo, *APL Mater.*, 2014, **2**, 081503.
17 L. Pop, F. Dumitru, N. D. Hadade, Y. M. Legrand, A. van der Lee, M. Barboiu and I. Grosu, *Org. Lett.*, 2015, **17**, 3494–3497.
18 T. Nakagawa, S. Y. Ku, K. T. Wong and C. Adachi, *Chem. Commun.*, 2012, **48**, 9580–9582.
19 C. Poriel, F. Barrière, D. Thirion and J. Rault-Berthelot, *Chem. – Eur. J.*, 2009, **15**, 13304–13307.
20 M. Romain, D. Tondelier, J.-C. Vanel, B. Geffroy, O. Jeannin, J. Rault-Berthelot, R. Métivier and C. Poriel, *Angew. Chem., Int. Ed.*, 2013, **52**, 14147–14151.
21 Y. Wu, J. Zhang, Z. Fei and Z. Bo, *J. Am. Chem. Soc.*, 2008, **130**, 7192–7193.
22 N. Harada, H. Ono, T. Nishiwaki and H. Uda, *J. Chem. Soc., Chem. Commun.*, 1991, 1753–1755.
23 J. Ramakrishna and P. Venkatakrishnan, *Chem. – Asian J.*, 2017, **12**, 181–189.
24 G. Gao, N. Liang, H. Geng, W. Jiang, H. Fu, J. Feng, J. Hou, X. Feng and Z. Wang, *J. Am. Chem. Soc.*, 2017, **139**, 15914–15920.
25 T. Wöhrle, I. Wurzbach, J. Kirres, A. Kostidou, N. Kapernaum, J. Litterscheidt, J. C. Haenle, P. Staffeld, A. Baro, F. Giesselmann and S. Laschat, *Chem. Rev.*, 2016, **116**, 1139–1241.
26 A. Narita, X.-Y. Wang and X. Feng, *Chem. Rev.*, 2016, **116**, 1139–1241; K. Müllen, *Chem. Soc. Rev.*, 2015, **44**, 6616–6643.
27 J. N. Smith, J. M. Hook and N. T. Lucas, *J. Am. Chem. Soc.*, 2018, **140**, 1131–1141.
28 H.-J. Yen, H. Tsai, M. Zhou, E. F. Holby, S. Choudhury, A. Chen, L. Adamska, S. Tretiak, T. Sanchez, S. Iyer, H. Zhang, L. Zhu, H. Lin, L. Dai, G. Wu and H.-L. Wang, *Adv. Mater.*, 2016, **28**, 10250–10256.
29 C. Zhang, Y. Liu, X.-Q. Xiong, L.-H. Peng, L. Gan, C.-F. Chen and H.-B. Xu, *Org. Lett.*, 2012, **14**, 5912–5915.
30 T. Fujikawa, D. V. Preda, Y. Segawa, K. Itami and L. T. Scott, *Org. Lett.*, 2016, **18**, 3992–3995.
31 K. Kato, Y. Segawa, L. T. Scott and K. Itami, *Angew. Chem., Int. Ed.*, 2018, **57**, 1337–1341.
32 C. L. Hilton, C. R. Jamison, H. K. Zane and B. T. King, *J. Org. Chem.*, 2009, **74**, 405–407.
33 T. M. Long and T. M. Swager, *Adv. Mater.*, 2001, **13**, 601–604.
34 C. Fan, Y. Chen, P. Gan, C. Yang, C. Zhong, J. Qin and D. Ma, *Org. Lett.*, 2010, **12**, 5648–5651.
35 R. E. Douthwaite, A. Taylor and A. C. Whitwood, *Acta Crystallogr., Sect. C: Cryst. Struct. Commun.*, 2005, **61**, O328–O331.
36 S. K. Pal, M. E. Itkis, F. S. Tham, R. W. Reed, R. T. Oakley, B. Donnadieu and R. C. Haddon, *J. Am. Chem. Soc.*, 2007, **129**, 7163–7174.
37 S. K. Pal, P. Bag, M. E. Itkis, F. S. Tham and R. C. Haddon, *J. Am. Chem. Soc.*, 2014, **136**, 14738–14741.
38 P. T. Herwig, V. Enkelmann, O. Schmelz and K. Müllen, *Chem. – Eur. J.*, 2000, **6**, 1834–1839.
39 R. Rathore and C. L. Burns, *J. Org. Chem.*, 2003, **68**, 4071–4074.
40 C.-Y. Tsai, Q. Zhang, Y.-Z. Wang, J. Shyong, H.-L. Chen and D.-J. Liaw, *Polym. Chem.*, 2017, **8**, 3327–3332.
41 R. Yamaguchi, S. Ito, B. S. Lee, S. Hiroto, D. Kim and H. Shinokubo, *Chem. – Asian J.*, 2013, **8**, 178–190.
42 M. Kastler, J. Schmidt, W. Pisula, D. Sebastiani and K. Müllen, *J. Am. Chem. Soc.*, 2006, **128**, 9526–9534.
43 P. J. Krusic and E. Wasserman, *J. Am. Chem. Soc.*, 1991, **113**, 2322–2323.